ORGANOMETALLICS

ARTICLE

pubs.acs.org/Organometallics

Stereoelectronic Factors in Iron Catalysis: Synthesis and Characterization of Aryl-Substituted Iron(II) Carbonyl P−N−N−P Complexes and Their Use in the Asymmetric Transfer Hydrogenation of Ketones

Peter E. Sues, Alan J. Lough, and Robert H. Morris*

Department of Chemistry, University of Toronto, Toronto, Ontario M5S 3H6, Canada

Supporting Information

ABSTRACT:

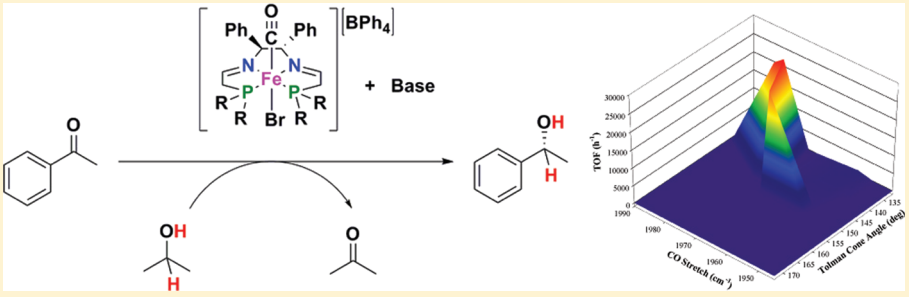

A series of five (*S*,*S*)-*trans*-[Fe(CO)(Br)(PR_2-CH_2CH=NCH(Ph)CH(Ph)N=$CHCH_2$-PR_2)][X] compounds (**1a**−**c**, X = BPh_4; **1d**,**e**, X = BF_4) were synthesized and tested for the asymmetric transfer hydrogenation (ATH) of acetophenone. Three of the complexes had methyl-substituted aryl groups (**a**, R = *para*-$CH_3C_6H_4$; **b**, R = *ortho*-$CH_3C_6H_4$; **c**, R = 3,5-$(CH_3)_2C_6H_3$), and two had trifluoromethyl-substituted aryl groups (**d**, R = *para*-$CF_3C_6H_4$; **e**, R = 3,5-$(CF_3)_2C_6H_3$). Using both known and new phosphonium dimers, [*cyclo*-$(PR_2CH_2CH(OH)-)_2$][Br]$_2$ (**2a**−**c**), in a one-pot template reaction, the corresponding (*S*,*S*)-*trans*-[Fe$(CH_3CN)_2$(PR_2-CH_2CH=NCH(Ph)CH(Ph)N=$CHCH_2$-PR_2)][BPh_4]$_2$ complexes (**3a**−**c**) were generated and then converted to precatalysts **1a**−**c** via CO addition reactions. While investigating compounds **1a**−**c**, an alternative route for synthesizing phosphonium dimers was developed that allowed the facile introduction of tetrafluoroborate counterions. Compounds **1d** and **1e** could not be synthesized using previously developed methods; phosphinoacetaldehyde diethyl acetal precursors (**5d**, **5e**) were isolated because trifluoromethyl-substituted phosphonium dimers did not form. Precursors **5d** and **5e** were incompatible with a base-catalyzed template approach, so a new acid-catalyzed template procedure was developed to generate the tetrafluoroborate salts (*S*,*S*)-*trans*-[Fe$(CH_3CN)_2$(PR_2-CH_2CH=NCH(Ph)CH(Ph)N=$CHCH_2$−PR_2)][BF_4]$_2$ (**3d**, **3e**). Both **3d** and **3e** were converted to precatalysts **1d** and **1e** via CO addition reactions. Complexes **1b**, **1d**, and **1e** were inactive for the ATH of acetophenone, while complexes **1a** and **1c** were active. Compound **1a** showed very high activity, with a turnover frequency of 30 000 h^{-1} at 28 °C, and is currently the most active iron ATH catalyst. Compound **1c** produced more enantiopure (*R*)-1-phenylethanol, with an ee of 90%, and is the most selective iron catalyst reported to date for the ATH of acetophenone. The activity of complexes **1a**−**e** for ATH was compared to those of known complexes **1f** (R = Ph), **1g** (R = Et), **1h** (R = *i*-Pr), and **1i** (R = Cy), and the most active catalysts were defined by a narrow range of electronic (ν(CO)) as well as steric (Tolman cone angles) parameters.

INTRODUCTION

Economic and political pressure for more sustainable, environmentally friendly practices has provided a driving force for the development of greener catalysts that incorporate cheap, abundant metals. Iron is an attractive candidate for replacing platinum group metals for these reasons; it is inexpensive, plentiful, and environmentally benign.[1] In fact, iron is an essential element that is found in the enzymes of every living system. Inspired by nature, many oxidation catalysts based on iron[2−7] were developed in the past, several of which employed macrocyclic ligands.[8−11] More recently, however, research focus has shifted toward reductive transformations, and many well-defined iron catalysts have been reported that have applications in commercially relevant reductions of polar bonds.[12,13] Several promising hydrosilylation,[14,15] direct hydrogenation,[16,17] and transfer hydrogenation (TH)[18−23] systems based on iron have been developed for the reduction of ketones, as well as imines.[24,25]

The asymmetric transfer hydrogenation (ATH) of prochiral ketones is a valuable transformation because it allows the

Received: June 16, 2011
Published: July 20, 2011

dx.doi.org/10.1021/om2005172 | *Organometallics* 2011, 30, 4418–4431

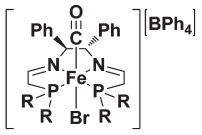

1a: R = *para*-$CH_3C_6H_4$
1b: R = *ortho*-$CH_3C_6H_4$
1c: R = 3,5-$(CH_3)_2C_6H_3$
1d: R = *para*-$CF_3C_6H_4$
1e: R = 3,5-$(CF_3)_2C_6H_3$
1f: R = Ph
1g: R = Et
1h: R = i-Pr
1i: R = Cy

Figure 1. Iron(II) carbonyl P−N−N−P complexes developed by Morris and co-workers for ATH.

synthesis of enantiopure alcohols for use in the pharmaceutical, fragrance, and food industries.[26,27] This field is dominated by systems that employ expensive as well as toxic platinum group metals,[28] such as the ruthenium and iridium ATH catalysts reported by Noyori[29] and Gao.[30,31] A common theme of these catalysts is that they employ ligands with two phosphorus donors and two nitrogen donors.[29] A particularly attractive ligand used by Gao and Noyori is a chiral tetradentate ligand, which coordinates via two phosphorus donors and two nitrogen donors (a P−N−N−P ligand).[32]

To date, the only iron catalysts that challenge platinum metal ATH catalysts on both activity and selectivity were developed by the Morris group.[33,34] These complexes utilize chiral P−N−N−P ligands different from those of Noyori's ruthenium catalysts in that they contain two imines and have only one methylene linker between the phosphorus and imine functionalities (see Figure 1).[34,35] Complex **1f** in particular is exceptional; when activated with base, it is the most active and selective iron ketone ATH catalyst reported thus far, with turnover frequencies (TOF) of 28 000 h^{-1} at 28 °C to give (*R*)-1-phenylethanol in 82% ee.[34] On the other hand, more hindered ketones, such as *tert*-butyl phenyl ketone, are reduced to alcohols in up to 99% ee.[34] The high activity and selectivity of **1f** has been attributed to the (*S*,*S*)-1,2-diphenylethylenediamine (*S*,*S*-dpen) backbone in combination with the phenyl substituents on the phosphorus donors.[34] With ethyl substituents on the phosphorus donors the catalyst **1g** is much less active and selective.[35]

Despite the high TOF and high enantioselectivity of complex **1f**, further improvements are needed to make iron catalysts competitive with existing ruthenium catalysts. Noyori and co-workers discovered that they could increase the activities of their ruthenium bis-chelate direct hydrogenation catalysts by replacing the phenyl groups on BINAP with more electron-donating *para*-tolyl groups.[29] In addition, for the same catalytic systems, as well as for related ATH systems reported by Morris and co-workers, it was found that replacing the phenyl groups with *meta*-xylyl groups afforded more enantiopure products.[29,36] Conversely, an increase in activity was seen for rhodium hydroformylation catalysts when electron-withdrawing groups were installed on the phosphorus donors, especially *para*- or 3,5-ditrifluoromethyl-substituted phenyl groups.[37,38] Furthermore, a similar trend was seen for rhodium arylation catalysts[39] and ruthenium oxidation catalysts,[40] as well as for a nickel asymmetric hydrocyanation catalyst, which also saw increased enantioselectivity with 3,5-ditrifluoromethyl-substituted phenyl groups.[41]

In this paper we explore the synthesis of a new series of iron(II) carbonyl P−N−N−P complexes containing methyl- and trifluoromethyl-substituted aryl groups and examine their activity for ATH. By tuning the steric and electronic properties of the complexes through their phosphorus donors while maintaining an *S*,*S*-dpen backbone, we endeavored to develop more active and selective catalysts. In addition, by comparing the catalytic activities of the electron-donating and -withdrawing groups it was anticipated we would gain some insight into the ATH mechanism. With respect to nomenclature, throughout this paper compounds will be named according to their aryl substitution pattern: **a** for *para*-tolyl; **b** for *ortho*-tolyl; **c** for *meta*-xylyl, **d** for *para*-trifluoromethylphenyl, and **e** for 3,5-ditrifluoromethylphenyl.

RESULTS AND DISCUSSION

Conventional Synthesis (Route A) of Phosphonium Dimers 2a−c. The new dimeric phosphonium salts **2b** and **2c** were synthesized according to a known literature procedure (Scheme 1, route A), which has already been successfully employed to generate **2a**.[42] Much like **2a**, the synthesis of **2b** and **2c** yielded air-stable, white solids in high yields (80−90%). The $^{31}P\{^1H\}$ NMR spectrum of **2c** showed two characteristic singlets: a major peak at 12.9 ppm and a minor peak at 14.8 ppm. These peaks indicate that both the *rac*- and *meso*-diastereomers of this compound are present.

Dimer **2b**, on the other hand, showed a dramatically different behavior in solution. The ^1H NMR spectrum of **2b**, in DMSO-d_6, showed three species in solution: an aldehyde (doublet of triplets at 9.6 ppm) and an enol (two doublets of doublets in a 1:1 integration ratio at 6.9 and 5.3 ppm) in a 1:2 ratio, as well as a very broad singlet around 12.3 ppm. The $^{31}P\{^1H\}$ NMR spectrum showed two sharp singlets at 25.1 (enol) and 28.1 ppm (aldehyde), indicating that both the enol and aldehyde phosphori were protonated and that interconversion of the two tautomers occurred relatively slowly. No coupling was observed, however, between phosphorus and hydrogen in the ^{31}P NMR spectrum. This can be explained if the protonated phosphori are in equilibrium with protonated DMSO and the rate of exchange between the two is similar or greater than the frequency of the coupling between the phosphori and hydrogen (approximately 500 Hz). This exchange process would also account for the broad singlet seen in the ^1H NMR spectrum, which corresponds to acid in solution. These findings are summarized in Scheme 2. Contrary to these findings, an IR spectrum of dimer **2b** (KBr disk) did not exhibit any characteristic absorptions for aldehydes or protonated phosphonium salts.

In another attempt to characterize **2b** in solution, additional NMR spectra of the compound were run in MeOH-d_4, which has a lower dielectric constant than DMSO. The spectra obtained were quite different than those run previously in DMSO-d_6. The $^{31}P\{^1H\}$ NMR spectrum revealed a very broad peak at −21.0 ppm, which suggests the presence of a three-coordinate phosphine in solution undergoing a dynamic process on a time scale near that of the NMR experiment. We believe this is a fast exchange of protons between the phosphorus and the solvent. In addition, both the $^{13}C\{^1H\}$ and ^1H NMR spectra of **2b** in CD_3OD were indicative of a hemiacetal, and the high-resolution ESI^+ MS (MeOH) spectrum showed a peak at 289.1 *m*/*z* for the protonated hemiacetal $[C_{19}H_{20}O_2P]^+$.

Further contradictions arose when examining the elemental analysis (EA) of **2b**, which was consistent with that of a dimer, and the high-resolution DART-MS (direct analysis in real time mass spectrometry) spectrum, which also gave evidence for a dimer with a peak at 257.1 *m*/*z* for the doubly charged species $[C_{32}H_{36}O_2P_2]^{2+}$. On the basis of the EA and DART-MS results,

dx.doi.org/10.1021/om2005172 |*Organometallics* 2011, 30, 4418–4431

Scheme 1. Conventional (Route A) and Alternative (Route B) Syntheses of Aryl-Substituted Phosphonium Dimers[a]

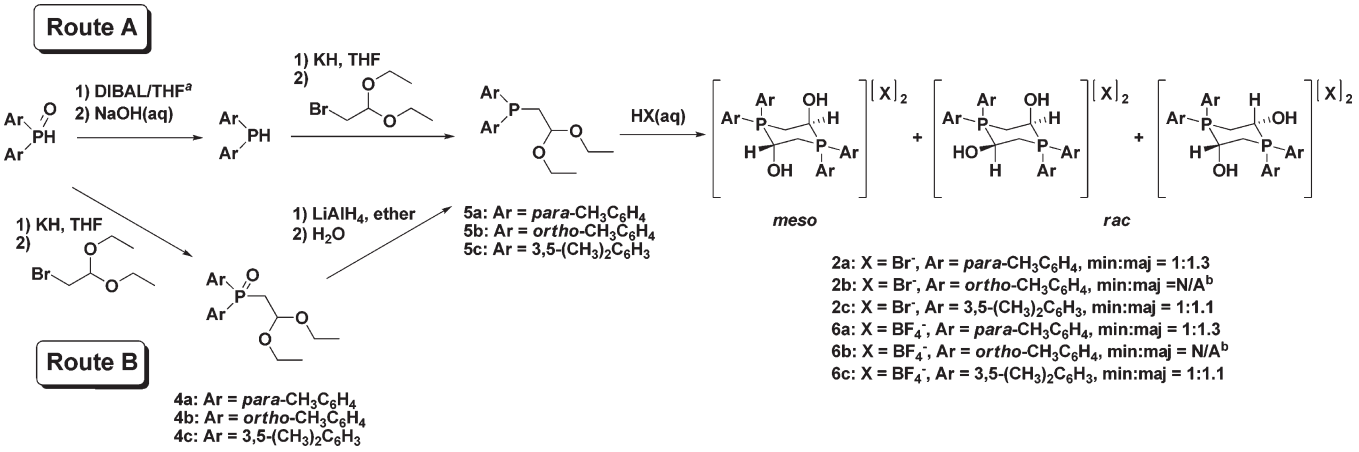

[a] DIBAL refers to diisobutylaluminum hydride, and THF refers to tetrahydrofuran. [b] N/A: not applicable. Dimers **2b** and **6b** decomposed upon dissolving in common NMR solvents, so the ratio of diastereomers could not be determined.

Scheme 2. Dynamic Behavior of Dimer 2b in DMSO and MeOH Solutions

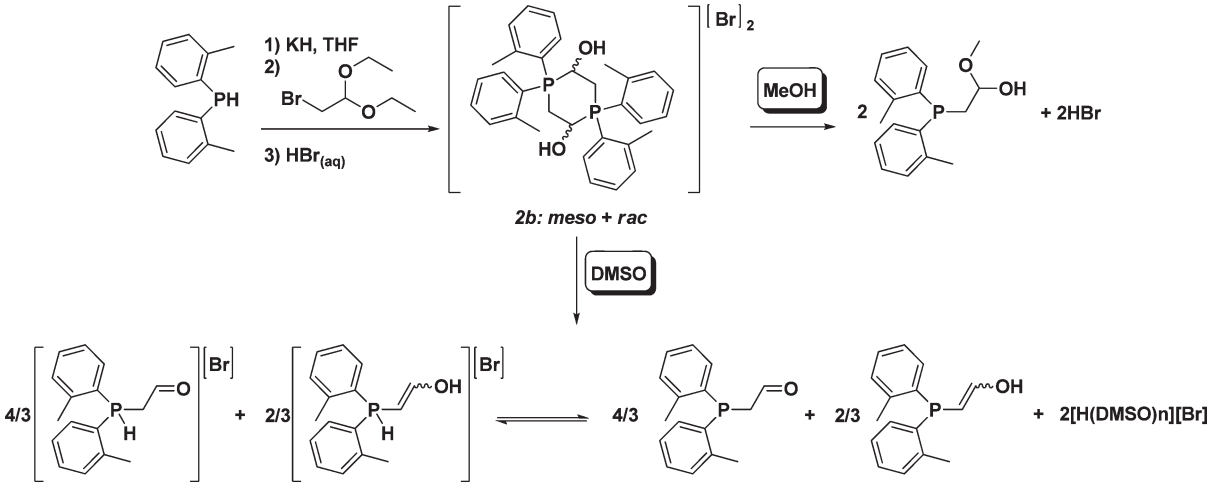

as well as the IR spectrum, we propose that **2b** is a phosphonium dimer. It is a kinetic product that quickly forms and precipitates out of solution, but decomposes upon dissolution to give products that depend on the nature of the solvent (summarized in Scheme 2).

Synthesis of Bis-acetonitrile Complexes 3a−c. Despite the peculiar behavior of dimer **2b**, all three of the aforementioned phosphonium dimers, **2a−c**, were successfully employed in the previously reported template synthesis of iron(II) P−N−N−P bis-acetonitrile complexes.[43,33] In a three-step, one-pot reaction, phosphonium dimer **2a**, **2b**, or **2c**, NaOMe, $[Fe(H_2O)_6][BF_4]_2$, and (*S*,*S*)-dpen were stirred in an CH_3CN/MeOH solution for several days at room temperature to yield the desired metal complexes **3a−c** (see Scheme 3). In the case of **3a** and **3b** this process took 1−2 days, while for **3c** it took 10−12 days. In order to accelerate conversion, the reaction mixture of **3c** was refluxed for several hours.

A salt metathesis reaction with $NaBPh_4$ was required to remove the mixture of counterions (Br^-, $FeBr_4^-$, and BF_4^-) present in the reaction mixtures of **3a−c**, and the complexes were

Scheme 3. One-Pot Template Synthesis of Complexes 3a−c

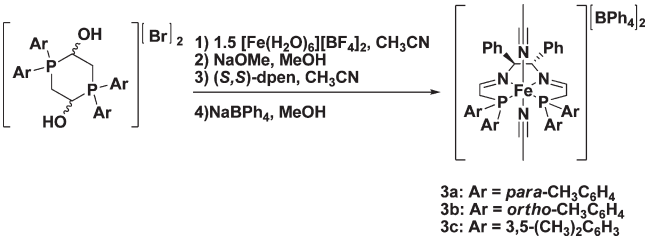

isolated as BPh_4^- salts. The yields of isolated products were poor, ranging from 10% to 37% due to the high solubility of the complexes. However the conversions were excellent without isolation, and these reaction mixtures were used directly in carbonylation reactions to produce **1a−c**.

Compounds **3a−c** all gave characteristic singlets in the $^{31}P\{^1H\}$ NMR spectra (61.7, 66.8, and 72.4 ppm for **3a**, **3b**, and **3c**,

dx.doi.org/10.1021/om2005172 |*Organometallics* 2011, 30, 4418–4431

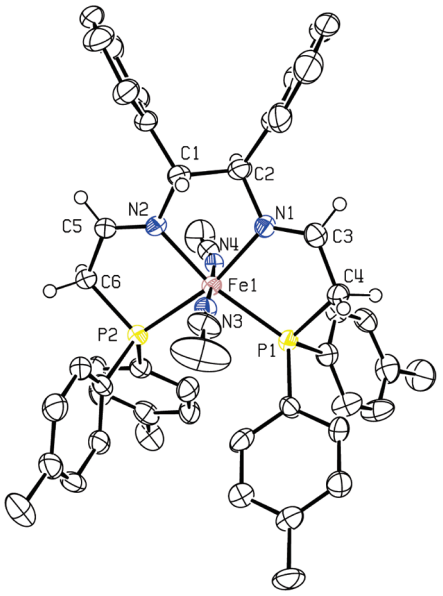

Figure 2. ORTEP3 representation (thermal ellipsoids at 50% probability) and atom numbering for **3a**. The solvent, counterion, and most hydrogens are omitted for clarity.

respectively) as well as imine peaks in the ^{1}H NMR spectra (around 8.2 ppm for **3a**−**c**). Furthermore, two sets of inequivalent methyl groups (around 2.2 ppm) were seen for all three complexes.

Crystals of **3a** as a tetrabromoferrate salt and a methanol solvate, suitable for X-ray diffraction studies, were grown from the slow diffusion of ether into an CH_3CN/MeOH solution of the crude reaction mixture. The geometry around iron in **3a**, shown in Figure 2, is a distorted octahedron with acetonitrile ligands in the apical positions *trans* to each other. The P−Fe−P angle is obtuse, 109.63(6)°, which suggests that the three five-membered rings formed by the tetradentate P−N−N−P ligand constrain the geometry of the metal center considerably. Other notable bond lengths and angles are given in Table 1. Another important feature of this structure is that the phenyl rings of the diamine backbone are equatorial, while the less sterically demanding hydrogens occupy the axial positions. Compound **3b** was also characterized by single-crystal X-ray diffraction and displayed a similar geometry (see Supporting Information, Figure S1).

Alternative Synthesis (Route B) of Phosphonium Dimers 2a−c and 6a−c. A drawback of synthetic route A (see Scheme 1) is that highly air-sensitive diarylphosphines are needed as starting materials. The literature synthesis of these compounds involves the use of Grignard reagents and diethyl phosphite to generate diarylphosphine oxides, which are subsequently reduced to phosphines using DIBAL.[44] The reduction step in this synthesis is tedious, labor intensive, and, in some cases, slow and low-yielding. This was the impetus for the development of an alternative, more convenient, and efficient method of synthesizing phosphonium dimers (Scheme 1, route B). In the first step, a diarylphosphine oxide is deprotonated and acts as a nucleophile to displace the Br^- of bromoacetaldehyde diethyl acetal in an S_N2 reaction. This affords diarylphosphine oxide acetaldehyde diethyl acetals **4a**−**c** as air-stable solids in moderate yields (60−75%). The $^{31}P\{^1H\}$ NMR spectra are diagnostic with singlets at 28.6, 30.1, and 28.7 ppm, for **4a**, **4b**, and **4c**, respectively. Furthermore, the ^{1}H NMR spectra for **4a**−**c** reveal a characteristic doublet of doublets around 2.7 ppm corresponding to the methylene protons *alpha* to phosphorus. The structure of **4b** was confirmed by single-crystal X-ray diffraction (see Supporting Information, Figure S2).

Table 1. Selected Bond Lengths (Å) and Angles (deg) for 3a

	3a·0.5MeOH
	Bond Lengths (Å)
Fe−P(1)	2.259(2)
Fe−P(2)	2.248(2)
Fe−N(1)	1.965(5)
Fe−N(2)	1.974(5)
Fe−N(3)	1.910(5)
Fe−N(4)	1.915(5)
	Bond Angles (deg)
P(1)−Fe−P(2)	109.63(6)
N(1)−Fe−N(2)	82.9(2)
N(3)−Fe−N(4)	177.6(2)
P(1)−Fe−N(1)	84.0(1)
P(1)−Fe−N(2)	165.9(2)
P(1)−Fe−N(3)	85.0(1)
P(1)−Fe−N(4)	97.3(1)
P(2)−Fe−N(1)	166.3(1)
P(2)−Fe−N(2)	83.7(1)
P(2)−Fe−N(3)	93.4(2)
P(2)−Fe−N(4)	85.0(1)

In the second step of route B, phosphine oxides **4a**−**c** are reduced to their corresponding phosphines, **5a**−**c**, using lithium aluminum hydride. Colorless oils of **5a**−**c** can be isolated in moderate yields (45−60%). Despite the limitations of the yield, this synthetic route has practical advantages: it is easy to set up and requires simple product workup. In addition, the crude product can be used directly to synthesize phosphonium dimers because all impurities present in the crude reagent are removed during dimer purification. Moreover, if a pure form of the phosphinoacetaldehyde diethyl acetal is desired, the crude product can be purified using a silica gel column in air. Unlike secondary diarylphosphines, compounds **5a**−**c** are only mildly air-sensitive, even in solution, and only begin to oxidize upon extended exposure to oxygen. The ^{1}H NMR spectra of **5a**−**c** were similar to those of **4a**−**c**, but the $^{31}P\{^1H\}$ NMR chemical shifts showed diagnostic peaks around −24.2 ppm for compounds **5a** and **5b** and −45.5 ppm for compound **5c**.

In the final step, crude products of **5a**−**c** were dissolved in THF and an excess of aqueous acid was added. After stirring overnight, phosphonium dimers **2a**−**c** or **6a**−**c** could be isolated as mixtures of *meso*- and *rac*-diastereomers in excellent yields (87−94%, see Scheme 1). The spectra of **2a**−**c** were identical to those of **6a**−**c**, and the structures of both **6a** and **6c** were determined by single-crystal X-ray diffraction (see Supporting Information, Figures S3 and S4). Much like **2a**, the isomers that were crystallized for **6a** and **6c** were *meso* with six-membered rings in the chair conformation.

The synthesis of BF_4^- salts **6a**−**c** demonstrates the utility of synthetic route B versus route A. In route B, any acid can be used to generate a phosphonium dimer from phosphines **5a**−**c** because the air-stable intermediates **4a**−**c** can be isolated free

Scheme 4. Template Synthesis of 3a−c Using 6a−c

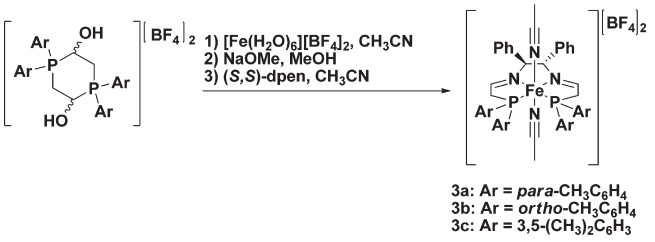

3a: Ar = *para*-$CH_3C_6H_4$
3b: Ar = *ortho*-$CH_3C_6H_4$
3c: Ar = 3,5-$(CH_3)_2C_6H_3$

of all halide salt byproduct. Conversely, in route A, only the use of aqueous HCl or HBr is practical, depending on the haloacetaldehyde diethyl acetal used in the synthesis because, otherwise, the product would have a mixture of counterions.[42,45] Thus, route B permits the facile introduction of a variety of counterions into the phosphonium salts and greatly increases their value as ligand precursors. Halide counterions can coordinate to transition metals and can compete with desired ligands to give unwanted side products. For example as illustrated in Scheme 3, an extra half-equivalent of iron(II) starting material is needed to accommodate the formation of $FeBr_4^{2-}$ when using a bromide salt of the phosphonium dimer.[43,33]

With a BF_4^- salt, however, the excess iron starting material is unnecessary, and the template synthesis is more atom-economical (see Scheme 4). With route B, phosphonium dimers can be tailored to different reaction conditions and metal pecursors by simply changing the acid used to generate them. This luxury is often lacking in synthetic inorganic chemistry, where it is generally the metal precursor that is changed when a reaction does not give the desired product, or a sacrificial reagent such as $AgBF_4$ is used to remove unwanted halides.

Synthesis of Precursors 5d and 5e, as Well as Bis-acetonitrile Complexes 3d and 3e. In addition to substituting the aryl groups on phosphorus with electron-donating methyl groups, efforts were made to substitute them with electron-withdrawing trifluoromethyl groups in the *para*- and 3,5-positions. Unfortunately, with these substituents, neither route A nor B gave the desired products. The strongly electron-withdrawing aryl groups reduced the nucleophilicity of the bonded phosphorus center to such an extent that it was unable to displace a bromide as a phosphine oxide anion in route B and unable to attack an aldehyde after acid addition as a trisubstituted phosphine in route A (summarized in Scheme 5).

Fortunately, the diarylphosphinoacetaldehyde diethyl acetals **5d** and **5e** could be synthesized cleanly if the temperature of the reaction mixture was controlled (see Experimental Section for details). Moreover, these compounds can be purified using silica gel chromatography in air because the oxidation potential of the phosphorus is raised by the electron-withdrawing substituents. To synthesize **5d** and **5e**, the corresponding diarylphosphine was deprotonated by KH in order to generate a potassium phosphide salt. After addition of bromoacetaldehyde diethyl acetal and workup, a dark oil was obtained in moderate yields (72−78%). Both **5d** and **5e** gave singlets in the ^{19}F NMR spectra at −63.3 ppm, as well as in the $^{31}P\{^1H\}$ NMR spectra at −22.0 and −19.0 ppm, respectively. The ^1H NMR spectra of **5d** and **5e** were very similar to those of compounds **5a−c**.

A problem arose when contemplating the use of diarylphosphinoacetaldehyde diethyl acetal precursors **5d** and **5e** in a templating reaction: these compounds have the opposite properties of phosphonium dimers. Whereas phosphonium dimers are stable with respect to acid and generate phosphinoacetaldehydes upon exposure to base, **5d** and **5e** are stable with respect to base and generate phosphinoacetaldehydes upon exposure to acid. The conventional template approach illustrated in Scheme 3 is base-catalyzed and thus is unsuitable for these starting materials. Instead, an acid-catalyzed templating approach was developed (see Scheme 6).

A diarylphosphinoacetaldehyde diethyl acetal precursor, **5d** or **5e**, was dissolved in CH_3CN with $[Fe(H_2O)_6][BF_4]_2$, followed by addition of *S*,*S*-dpen. A small amount of aqueous HBF_4 was subsequently introduced into the system in order to deprotect **5d** or **5e** and generate a diarylphosphinoacetaldehyde *in situ*. The solution was then neutralized with NaOMe, and upon workup, dark red solids could be isolated in moderate yields (45−50%). Both **3d** and **3e** showed characteristic singlets in their $^{31}P\{^1H\}$ NMR spectra at 69.0 and 72.0 ppm, respectively, as well as distinctive imine peaks in the ^1H NMR spectra around 8.2 ppm. A notable difference between **3d** and **3e** and their electron-donating counterparts **3a−c** was that there were no inequivalent methyl peaks in the ^1H NMR spectra. Instead, two inequivalent trifluoromethyl peaks were evident in the ^{19}F NMR spectra (at −63.4 and −63.6 ppm). It is interesting to note that the singlets in the $^{31}P\{^1H\}$ NMR spectra and the imine peaks in the ^1H NMR spectra of **3d** and **3e** were not shifted upfield by a significant amount relative to those of **3a−c**, indicating that these chemical shifts are insensitive to the electronic changes made at phosphorus.

The mechanism of the acid-catalyzed template synthesis is still poorly understood. Throughout the reaction, before arriving at the final product, the major peak in the $^{31}P\{^1H\}$ NMR spectra is a broad singlet around −10.1 ppm. This seems to indicate that the phosphorus is at most loosely bound to the iron, rapidly associating and dissociating such that this peak appears at the average of the chemical shifts of bound and unbound phosphorus. In addition, the reagents were added in several different sequences, but the given permutation was the only procedure that yielded the desired product. If diamine addition is withheld until after neutralization with base, a mixture of products is generated. If, on the other hand, the deprotection of **5d** or **5e** is attempted in the presence of both iron(II) and diamine, neutralization of the solution yields the desired P−N−N−P complex **3d** or **3e**.

It is surprising that deprotection of **5d** or **5e** must occur in the presence of both iron(II) and diamine because protonation of the basic diamine will occur rapidly upon addition of acid to this mixture. The protonated diamine, however, can act as a weak acid and deprotect the diarylphosphinoacetaldehyde diethyl acetal. After the diethyl acetal is deprotected, iron can act as a Lewis acid to increase the electrophilicity of the carbonyl carbon and facilitate Schiff base reactions. The amount of acid added is only enough to protonate each diamine once, so attack on the carbonyl carbon by the unprotonated amino group of the diamine would form a protonated tridentate ligand. This could explain the $^{31}P\{^1H\}$ NMR spectrum because a protonated tridentate ligand with an electron-deficient phosphorus donor would be prone to dissociation. After deprotonating the proposed tridentate ligand, it could coordinate to iron, forming complex **7**, which was characterized by X-ray crystallography (see Supporting Information, Figure S5). Upon further condensation with another equivalent of diarylphosphinoacetaldehyde, **7** could

dx.doi.org/10.1021/om2005172 |*Organometallics* 2011, 30, 4418–4431

Scheme 5. Synthesis and Lack of Reactivity of Trifluoromethyl-Substituted Precursors 5d and 5e

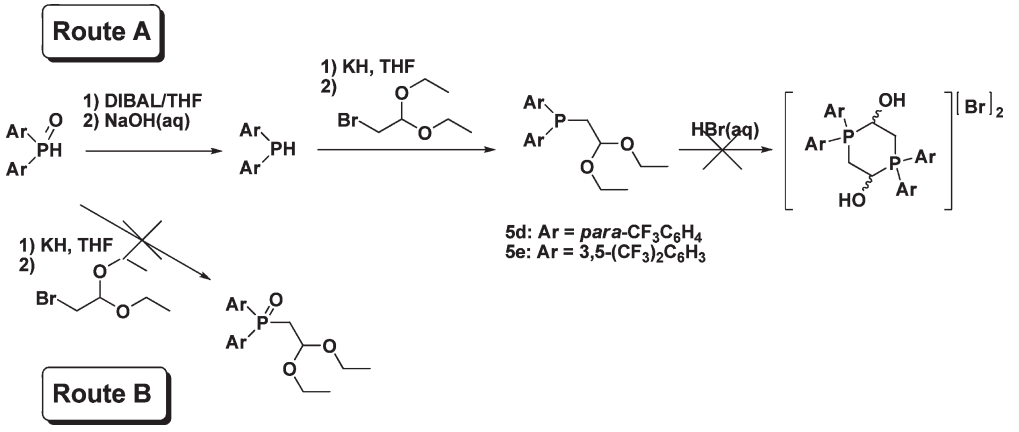

Scheme 6. Acid-Catalyzed Synthesis of 3d and 3e

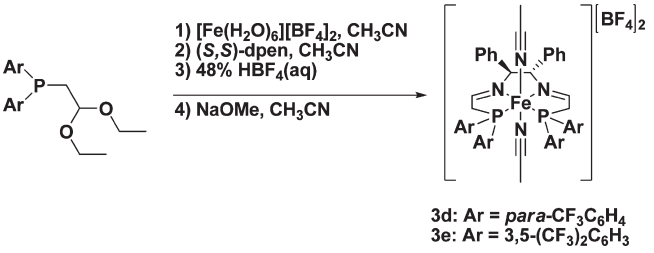

generate **3e** (summarized in Scheme 7). Presumably, the tridentate ligand is too sterically demanding to allow the formation of a bis-tridentate ligand complex, as was reported previously by our group.[43,46]

The acid-catalyzed deprotection of a precursor in the presence of a template is not an unfamiliar concept. This type of synthesis is used extensively by materials chemists in the preparation of mesoporous silica.[47] Acid is used to hydrolyze alkoxy-silane precursors in the presence of a liquid crystal template in order to produce silica with periodic channels.[47] This synthetic approach, however, is completely unknown in inorganic chemistry, where, in general, an acid-catalyzed template synthesis refers to a Lewis-acid-catalyzed process.[48] In addition, there are several Brønsted-base-catalyzed template syntheses known,[43,46,49,50] but the literature on Brønsted-acid-catalyzed templating is nonexistent. With the success of this process, a whole new range of compounds can be targeted for ligand synthesis, especially those that form unstable species upon treatment with acid. Under templating conditions, these species can be generated *in situ* and used to produce previously unknown series of ligands.

Synthesis of Iron(II) Carbonyl P−N−N−P Complexes 1a−e. The new iron(II) carbonyl complexes **1a−c** were synthesized according to a known literature procedure,[35,34] while small changes were made to generate complexes **1d** and **1e** (see Scheme 8). For **1a−c** the CO addition reaction was performed in acetone in the presence of an excess of KBr, and after several days, the products were isolated as BPh_4^- salts in low yields (10−35% overall with respect to the phosphonium dimer precursors).

The bis-acetonitrile intermediates used to generate **1a−c** were not isolated in order to reduce the number of purification steps and to increase atom economy.[35]

For **1d** and **1e**, on the other hand, the CO addition reaction was performed in CH_2Cl_2 with only one equivalent of KBr. The reaction progressed very slowly, taking over a week to proceed to completion, and required several cycles of solvent removal under reduced pressure, followed by addition of fresh solvent to remove any traces of CH_3CN from solution. The products, yellow solids, were isolated as BF_4^- salts in moderate yields (40−50%). Dichloromethane was chosen over acetone to prevent decomposition of **3d** and **3e**, and only one equivalent of KBr was used in order to prevent the formation of a mixture of products. The formation of **1d** and **1e** proceeded slowly undoubtedly because of the electron-deficient nature of the iron. Without much electron density to π back-donate into the CO ligand, the iron−carbon bond is much weaker. This would make other, more basic ligands, such as CH_3CN or Br^-, more competitive for coordination sites than CO and explains why the stoichiometry of KBr needs to be controlled as well as why the CH_3CN needs to be continually removed from the system.

Indeed, the electron-deficient nature of the iron in complexes **1d** and **1e** compared to **1a−c** is reflected in the CO vibrations listed in Table 2, which also lists the CO vibrations for literature complexes **1f−i** (see Figure 1 for structures), in addition to the steric parameters of the substituted phosphorus donors of **1a−i**. There is a 15−20 wavenumber difference between the CO vibrations of the approximately isosteric complexes with electron-donating and electron-withdrawing substituents, while there is a 45 wavenumber range overall for **1a−i**. The difference in wavenumber, however, is not reflected in the $^{31}P\{^1H\}$ NMR spectra. All of the CO complexes show diagnostic pairs of doublets between 60.0 and 70.0 ppm. An interesting feature to note for **1c** is that the $^{31}P\{^1H\}$ NMR spectrum shows an extreme second-order pattern at 61.3 ppm. Additionally, **1b** exhibits no phosphorus peaks at room temperature. This is due to limited rotation of the *ortho*-methyl-substituted aryl groups about the phosphorus donors as well as fast interconversion of rotoisomers on the time scale of the NMR experiment. If the spectrum is acquired at low temperatures, four sets of doublets appear: one major set, one minor set, and two sets with similar, intermediate intensities. This indicates there are four rotoisomers in solution with slightly different energies. The $^{31}P\{^1H\}$

dx.doi.org/10.1021/om2005172 |*Organometallics* 2011, 30, 4418–4431

Scheme 7. Proposed Mechanism for the Formation of 3e Using the Acid-Catalyzed Template Approach

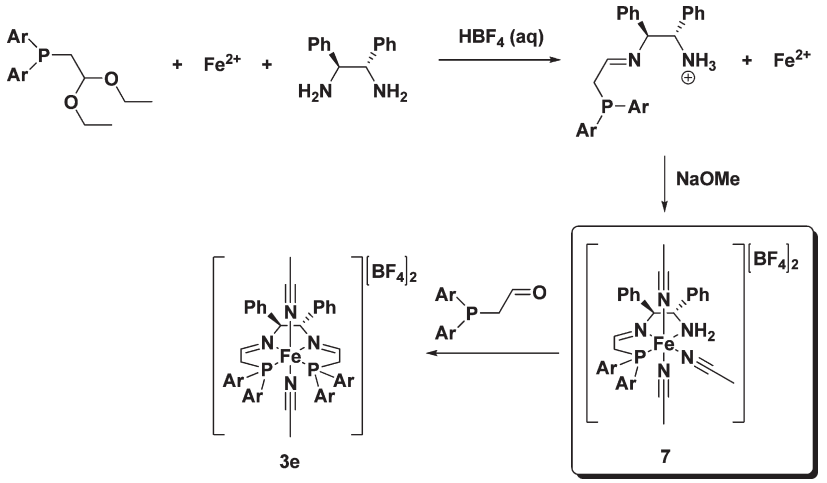

Scheme 8. General Method for Synthesizing 1a−e

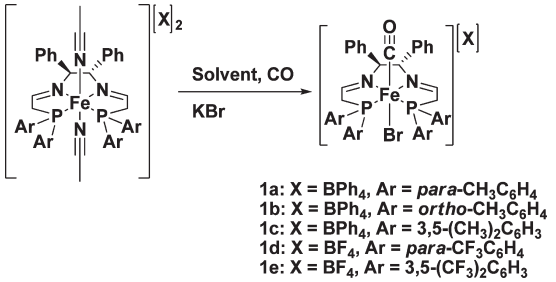

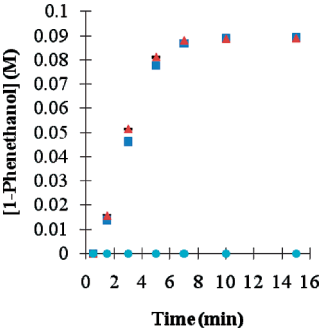

Figure 3. Reaction profiles of the ATH of acetophenone to (*R*)-1-phenylethanol using **1a**−**e**, in *i*PrOH, and in the presence of KO^{t}Bu. C/B/S = 1:8:1000, T = 28.2 °C, [Fe] = 92.4 μM. (■) **1a**, ee = 84%; (▲) **1c**, ee = 90%; (●) **1b**, **1d**, and **1e**. Each data point represents the average of three runs, and error bars are smaller than the symbols themselves.

NMR spectra of all the CO complexes show pairs of doublets due to the C_1 symmetry produced by the chiral *S*,*S*-dpen backbone and the different *trans* ligands on iron. This lack of symmetry also manifests in the ^{1}H and ^{19}F NMR spectra of **1a**−**e**. For **1a**−**c**, the methyl substituents are inequivalent and four methyl peaks around 2.1 ppm can be seen (for **1b**, there are 16 methyl peaks: four for each roto-isomer). The trifluoromethyl-substituted complexes **1d** and **1e** show a similar set of four peaks but in the ^{19}F NMR instead (around −63.5 ppm).

ATH Using Precatalysts 1a−e. We have previously shown that by replacing the phenyl groups on phosphorus with alkyl groups, the catalytic activity of the iron(II) carbonyl complexes for the ATH of ketones is either completely deactivated (**1h** and **1i**) or drastically decreased (**1g**).[35] It was believed that the steric bulk of the cyclohexyl and isopropyl groups was the cause of this deactivation, but it was difficult to definitively conclude whether or not this was true because these groups impose drastic electronic as well as steric effects.[35] Furthermore, the catalysts with less sterically demanding ethyl substituents showed only modest turnover frequencies at elevated temperatures, illustrating that electronic factors are playing a role in the lower activity of the alkyl complexes.[35]

In order to clearly separate the electronic from the steric effects, we prepared complexes with *ortho*- and *para*-substituted phenyl groups on the phosphorus donors. In this way, the electronics of the two systems would be very similar, but the steric crowding about the iron center would be drastically different. The *para*-methyl-substituted system, **1a**, showed high activity and selectivity for the asymmetric hydrogenation of acetophenone, while the *ortho*-methyl-substituted system, **1b**, was completely inactive (see Figure 3).

One possible mechanism of action for these catalysts was thought to be the dissociation of a phosphorus donor to create an open site for substrate coordination so that reduction could occur in a Meerwein−Ponndorf−Verley fashion.[51] This seems unlikely, though, in light of the inactivity of **1b**. The increased steric bulk around the phosphorus donors should favor dissociation, and indeed, the catalytic mixture displays numerous peaks in the negative region of the ^{31}P{^{1}H} NMR spectrum. Thus we conclude that under catalytic conditions the decoordination of phosphorus donors for **1b** occurs, but instead of leading to an active catalytic species, this process leads to numerous decomposition products.

We also synthesized a *meta*-xylyl version of our catalyst, **1c**, in the hopes that the increased steric bulk of these groups, which is slightly removed from the metal center, would afford more enantiopure products. Whereas **1a** produced (*R*)-1-phenylethanol with an ee of 84%, very similar to the 82% ee previously reported for **1f**, **1c** gave an improved ee of 90% for the production of (*R*)-1-phenylethanol. Only a few other catalysts produce such

Table 2. IR CO Stretches and Tolman Cone Angles of Iron(II) Carbonyl Complexes 1a−i

compound	substituent on phosphorus	CO stretch (cm^{-1})	cone angle[a] (deg)	ref
1i	cyclohexyl	1945	157	35
1g	ethyl	1951	132	35
1h	isopropyl	1956	151	35
1c	3,5-$(CH_3)_2C_6H_3$	1970	148[b]	this work
1a	*para*-$CH_3C_6H_4$	1972	141	this work
1b	*ortho*-$CH_3C_6H_4$	1974	173	this work
1f	phenyl	1975	141	34
1d	*para*-$CF_3C_6H_4$	1989	141	this work
1e	3,5-$(CF_3)_2C_6H_3$	1990	148[b]	this work

[a] Tolman cone angles for the phosphorus donors were calculated using parameters from Tolman (ref 52), Giering et al. (ref 53), and Poë and co-workers (ref 54) (see Supporting Information for sample calculations). The linkage between the phosphorus and imine moieties is modeled as an ethyl group. [b] Cone angles approximated from crystal structure 7. The Fe−P bond length is 2.22 Å for 7, which is close to the 2.28 Å Ni−P bond length in the model Ni^0 complex used to determine Tolman cone angles (ref 52). Note that this is a tentative estimate for both **1c** and **1e** (we approximate that CF_3 and CH_3 are similar in size).

high enantioselectivities for the ATH of unsubstituted acetophenone, and none are as active as **1c** (see Table 3).[28] Generally, such high ee are observed with other, bulkier ketones, with isopropyl or *tert*-butyl groups, as was seen by our group while screening substrates for **1f**.[33] For all of our iron(II) carbonyl catalysts, however, the ee begins to drop after approximately 10 minutes. More studies are underway to determine the nature of this loss of enantioselectivity.

We propose that all of the aforementioned active catalysts operate under the same mechanism because of some key similarities: they all have distinctive sigmoidal reaction profiles, and they all show the same color changes upon activation. In Figure 3, the reaction profiles of **1a** and **1c** show a brief induction period followed by a linear increase in product formation, which then tapers off as the concentration of substrate decreases and the system reaches equilibrium. This is consistent with results previously reported for **1f**.[34] Furthermore, **1a** and **1c** need to be activated by a strong base to be catalytically active, and upon reacting with base, the compounds turn green in color. This colored transition is also seen with the alkyl-substituted catalysts where a doubly deprotonated, five coordinate, bis-ene-amido iron(II) carbonyl complex was recently identified.[55] Yet another result in support of this proposal is that inactive **1b** does not turn green upon reacting with base. Instead, the solution turns nearly colorless as the complex decomposes.

After determining that substitutions in the *ortho*-position led to inactive catalysts and substitutions in the 3,5-positions led to increased selectivity, we rationalized that some mechanistic insights might be obtained if substitutions were made with electron-withdrawing trifluoromethyl groups in the para- and 3,5-positions. Precatalysts **1d** and **1e** were tested for activity under similar conditions to **1a**−**c**, but much to our surprise, these catalysts were completely inactive. If the mechanism involves transferring a hydride equivalent to an iron intermediate, **1d** and **1e** should favor and stabilize these species due to the electron-deficient nature of the metal center, but an increase in activity is not seen. In fact, upon addition of base to **1d** or **1e**, they do not turn green in color; instead, they turn orange. IR spectra of these reaction mixtures indicated that the CO ligand was still present after the base was added. We are currently exploring the reasons why **1d** and **1e** are completely inactive for the ATH of acetophenone.

After determining that **1a** and **1c** were active for the ATH of acetophenone, they were compared directly, under identical catalytic conditions, to **1f**. The initial rates of **1a**, **1c**, and **1f** were determined using high substrate loadings in order to saturate the catalysts and ensure a linear increase in product formation for an extended period of time (see Figure 4).

The TOF of **1f** was an impressive 28 000 ± 200 h^{-1}, with an ee of 82% as previously reported.[46] The TOF of isosteric **1a** was even higher, at 30 000 ± 1500 h^{-1} with an ee of 84%, while the TOF of **1c** was slightly lower at 26 000 ± 1000 h^{-1} with an elevated ee of 90%.

A striking and peculiar feature of the behavior of **1a** and **1c** stands out when Figures 3 and 4 are examined closely. In Figure 3, if **1a** and **1c** are compared, it is evident that **1c** is slightly faster. In Figure 4, on the other hand, **1a** is faster. This result seems somewhat counterintuitive at first; by increasing the concentration of substrate, the rate of **1c** does not increase as much as the rate of **1a**. If both systems operate under the same mechanism, this observation could be explained by a larger equilibrium constant for the formation of an inactive enolate complex for **1c** than for **1a**. This explanation is not favored, however, because transfer hydrogenation was conducted using benzophenone as the substrate, which cannot form an enolate, and the results showed that the rate of **1c** still had a lower dependence on the concentration of substrate than **1a** when increasing the substrate loading 6-fold (see Supporting Information, Figures S6−S11). The mechanism of ATH is still under investigation, and further studies may elucidate the cause of this interesting behavior.

Complexes **1a**, **1c**, and **1f** were all exceptionally active, but there does not seem to be a dramatic difference between them. We previously reported that electron-rich, alkyl-substituted phosphorus donors inhibited catalysis, yet **1a** is more active than **1f**, and **1c** is only slightly slower, which is surprising, as both **1a** and **1c** should be more electron-donating than **1f**. The IR spectra, however, show that catalysts **1a**, **1c**, and **1f** have similar carbonyl stretches (see Table 2), indicating that the iron centers have comparable electron densities. It is only when the carbonyl stretches vary drastically from these three complexes, as with **1d** and **1e** or the alkyl-substituted complexes **1g**−**i** (see Table 3), that the activity decreases drastically or disappears entirely.

In general, it seems that our iron(II) carbonyl catalysts require a delicate balance of both sterics and electronics at phosphorus to keep them active, as well as selective. If they are too electron-rich, their activity begins to drop, but if the compounds are too electron-deficient, they are completely inactive. At the same time,

Table 3. Comparison of Activity, Selectivity, and Reaction Conditions between 1c and Several Highly Selective Platinum-Metal-Based ATH Catalysts Reported in the Literature[a]

catalyst	S/C	temp (°C)	yield (%)/time	% ee	ref
1c/base	1000	28	94/7 min	90	this work
$[RuCl_2(mes)]_2$/Tsdpen/base	200	22	95/15 h	97	56
$RuCl_2$(**8**)/base	200	45	93/7 h	97	32
$[RuCl_2(hmb)]_2$/**9**/base	200	28	94/1 h	92	57
$[RuCl_2(p\text{-cym})]_2$/**10**/base	200	22	92/1.5 h	94	58
$[RuCl_2(p\text{-cym})]_2$/**11**/base	100	22	70/1.5 h	91	59
RuCl(**12**)/base	200	28	>99/18 h	96	60
Cp*RhCl(Tsdpen)/base	100	22	80/48 h	90	23
Cp*RhCl(Tscydn)/base	200	30	85/12 h	97	61
Cp*IrCl(Tscydn)/base	200	30	36/12 h	96	61
$[RuCl_2(p\text{-cym})]_2$/**13**/base	100	22	96/48 h	94	62
RuHCl(xylbinop)(dpen)/base	100	20	97/3 h	92	63
$RuH(BH_4)$(xylbinop)(dpen)	100	22	92/8 h	93	36

[a] Where the ligands are abbreviated as.

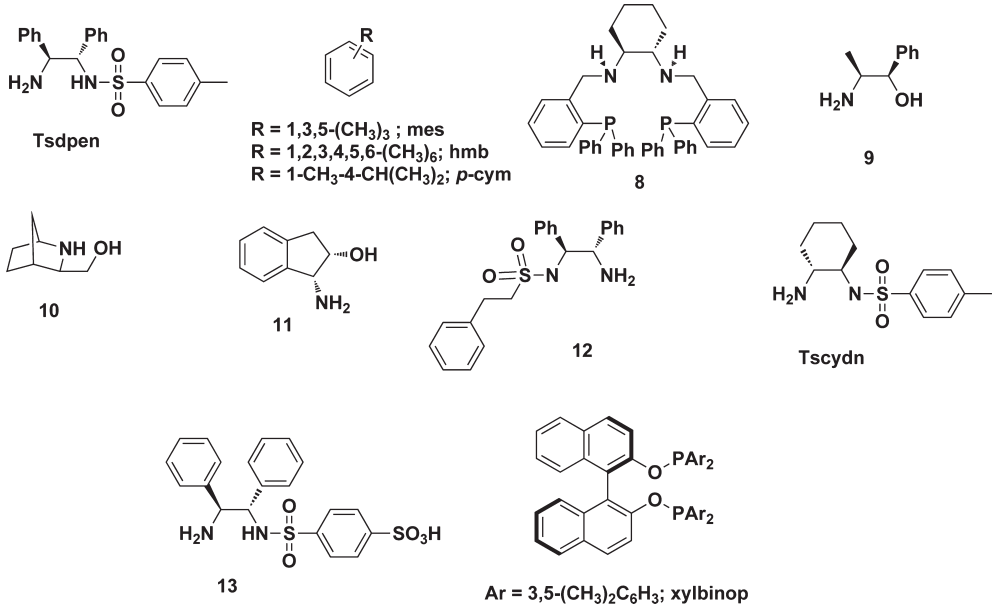

if they are too sterically hindered, they become completely inactive, but if they are not sterically hindered enough, the enantioselectivity of the catalysts drops significantly. This delicate balance of stereoelectronics can be represented graphically by plotting the catalytic activity of the iron complexes, in TOF, against CO stretching frequencies and Tolman cone angles (see Figure 5). This distinctive plot, a "volcano plot", reveals a narrow region of steric and electronic parameters that produces highly active ATH catalysts. Deviation from this region leads to completely inactive catalysts or severely diminished activity in the case of **1g**.[35] The phenyl groups, as well as *para*-methyl- and 3,5-dimethyl-substituted phenyl groups, must provide the right balance of sufficient Lewis basicity and steric bulk on the phosphorus donors to ensure fast turnover and high selectivity, but not so much electron density that the active species becomes too electron-rich to effectively abstract a hydrogen equivalent from *i*-PrOH.

"Volcano plots" have been extensively used to understand and design systems in heterogeneous catalysis.[64−66] In this case, however, the system is homogeneous, and the metal center is kept constant, while the phosphorus donors (L) are varied. Similar studies were conducted by Giering et al.[53] and Poë et al.,[54] where the steric and electronic effects of the phosphorus donors on the reduction potentials of η^5-Cp(CO)(L)Fe-(COMe) and the fragmentation of $Os_3(CO)_9(\mu\text{-}C_4Ph)$(L) were examined, respectively. In both studies, the influence of the stereoelectronic factors of the phosphorus donors on the transition states of these processes was explored in a qualitative manner. The approach in this paper is somewhat unique in that the activity of a catalytic system is examined with respect to both steric and electronic parameters on phosphorus donors. Rajanbabu et al.[41,67−69] and Gebbink et al.[70] have performed analogous studies with respect to the influence of phosphorus donors on catalytic activity, except that only electronic parameters were examined in the first case, and a qualitative approach regarding activity was used in the latter case. In the current work the TOFs of the catalysts, which are dictated by the transition states of the

dx.doi.org/10.1021/om2005172 |*Organometallics* 2011, 30, 4418–4431

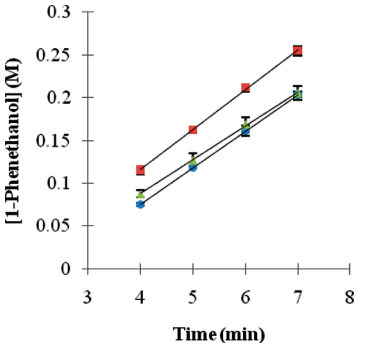

Figure 4. Linear, initial portions of the ATH of acetophenone to (*R*)-1-phenylethanol using **1f**, **1a**, and **1c**. C/B/S = 1:8:6000, *T* = 28.2 °C, [Fe] = 92.4 μM. (■) **1a**, ee = 84%; (▲) **1c**, ee = 90%; (●) **1f**, ee = 82%. Each data point represents the average of three runs.

rate-limiting steps, are compared to the stereoelectronic factors of the phosphorus donors. This type of analysis, in conjunction with density functional theory (DFT) and kinetic data, can be used to gain insights into the nature of the transition state of the rate-determining step for catalytic cycles. Moreover, with this type of analysis, "hot-spots" for activity can be identified and targeted for future ligand design and catalyst optimization.

■ CONCLUDING REMARKS

We have synthesized a series of five aryl-substituted iron(II) carbonyl P−N−N−P compounds and tested them for the ATH of prochiral ketones. Three of these complexes, **1a**, **1b**, and **1c**, had electron-donating methyl groups in the *para*-, *ortho*-, and 3,5-positions, respectively, while the other two complexes, **1d** and **1e**, had electron-withdrawing trifluoromethyl groups in the *para*- and 3,5-positions, respectively. Compounds **1a**−**c** were synthesized according to known literature procedures: starting with phosphonium dimers, **2a**−**c**, the bis-acetonitrile complexes, **3a**−**c**, were generated in a one-pot template synthesis and converted to precatalysts in a CO addition reaction. While investigating the methyl-substituted compounds, an alternative and more convenient route for synthesizing phosphonium dimers was developed, which allows facile introduction of any desired counterion, thus making the phosphonium dimers more synthetically useful and valuable. Compounds **1d** and **1e**, on the other hand, could not be synthesized using previously developed methods. Phosphonium dimers of the electron-withdrawing groups could not be isolated, so phosphinoacetaldehyde diethyl acetal precursors, **5d** and **5e**, were isolated instead. These precursors were incompatible with the previously reported template synthesis, so an unprecedented one-pot, acid-catalyzed template procedure was developed to generate bis-acetonitrile complexes **3d** and **3e**. Although the mechanism of the acid-catalyzed template is not completely known, it may go through a tridentate, trisacetonitrile intermediate. Compounds **3d** and **3e** were then converted to precatalysts in a standard CO addition reaction. Of the five CO compounds synthesized, only **1a** and **1c** were active catalysts; **1b** had too much steric crowding about the iron center, while **1d** and **1e** were too electron-poor. Complexes **1a** and **1b** were very successful: **1a** showed increased activity compared to **1f** and is now the most active iron ATH catalyst reported to date, while **1c** produced more enantiopure (*R*)-1-phenylethanol with an ee of 90% and is now the most selective iron ATH catalyst developed thus far. The activity of complexes

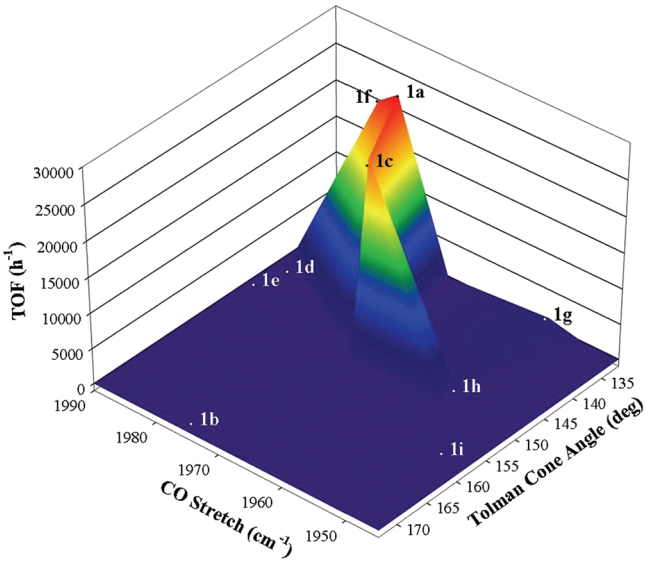

Figure 5. "Volcano plot" of catalyst activity (TOF, h^{-1}) versus CO stretch (cm^{-1}), as an electronic parameter, and Tolman cone angle (deg), as a steric parameter, for precatalysts **1a**−**i**.

1a−**e** for ATH was compared to the activities of previously reported complexes **1f**−**i**, and the most active catalysts displayed a narrow range of electronic and steric parameters for their phosphorus donors, as defined by CO stretches and Tolman cone angles, respectively. This analysis may give insights into the mechanism of catalysis and lead to more rational catalyst design.

■ EXPERIMENTAL SECTION

General Considerations. All procedures and manipulations were performed under an argon or nitrogen atmosphere using standard Schlenk-line and glovebox techniques unless stated otherwise. All solvents were degassed and dried using standard procedures prior to all manipulations and reactions unless stated otherwise. The synthesis of the *para*-methyl-substituted phosphonium dimer **2a** has previously been reported.[71] Deuterated solvents were purchased from Cambridge Isotope Laboratories or Sigma Aldrich, degassed, and dried over activated molecular sieves prior to use. All other reagents were purchased from commercial sources and utilized without further purification. The IR spectra of the KBr pellets containing precatalysts **1a**−**i** were measured on a Paragon 500 spectrometer (spectral range 4600 to 400 cm^{-1}) at 25 °C using Perkin-Elmer's SPECTRUM for data collection and processing. The ESI-MS data were collected on an AB/Sciex QStar mass spectrometer with an ESI source, the EI-MS data were collected on a Waters GC ToF mass spectrometer with an EI/CI source, and the DART-MS data were collected on a JEOL AccuTOF-DART mass spectrometer with a DART-ion source (no solvent is required). NMR spectra were recorded at ambient temperature and pressure using a Varian Gemini 400 MHz spectrometer (400 MHz for ^{1}H, 100 MHz for ^{13}C, 376 MHz for ^{19}F, and 161 MHz for ^{31}P) unless stated otherwise. The ^{1}H and ^{13}C NMR were measured relative to partially deuterated solvent peaks but are reported relative to tetramethylsilane. All ^{19}F chemical shifts were measured relative to trichlorofluoromethane as an external reference. All ^{31}P chemical shifts were measured relative to 85% phosphoric acid as an external reference. The elemental analyses were performed at the Department of Chemistry, University of Toronto, on a Perkin-Elmer 2400 CHN elemental analyzer. Some complexes gave inconsistent carbon analyses but acceptable hydrogen and nitrogen

dx.doi.org/10.1021/om2005172 |*Organometallics* 2011, 30, 4418–4431

contents; we attribute this to a combustion problem due to boron-containing counterions.[72]

Synthesis of $[C_{32}H_{36}O_2P_2][Br]_2$ (2b). A Schlenk flask was charged with KH (0.379 g, 9.5 mmol) and dry THF (9.5 mL). Di-(*ortho*-tolyl)phosphine (1.688 g, 7.9 mmol) was added, and the solution turned red in color. The solution was stirred for 90 min and then cooled to −78 °C. Bromoacetadehyde diethyl acetal (1.22 mL, 10.9 mmol) was added over 20 min, and the solution turned yellow. The solution was warmed to room temperature, and 48% HBr (1.8 g, 10.7 mmol) was added. A white precipitate formed and the solution turned colorless. The mixture was left stirring for 2 h and then placed in a freezer (−40 °C) overnight. The precipitate was filtered off and washed with H_2O (2 × 15 mL), as well as ethyl acetate (15 mL). The precipitate was dried under high vacuum. Yield: 83.1% (1.69 g). ^{1}H NMR (400 MHz, DMSO-d_6) δ: 12.60−12.05 (vb s, 3H), 9.59 (dt, 2H, Ar-H, J = 3.3, 1.1 Hz), 7.65 (ddd, 4H, Ar-H, J = 13.7, 7.7, 1.3 Hz), 7.54 (ddd, 2H, Ar-H, J = 13.7, 7.6, 1.4 Hz), 7.47 (tt, 4H, Ar-H, J = 7.5, 1.5 Hz), 7.41 (tt, 2H, Ar-H, J = 7.5, 1.4 Hz), 7.36−7.24 (m, 10H, Ar-H), 7.24−7.13 (m, 2H, Ar-H), 6.91 (dd, 1H, OHC*H*═CH, J = 13.1, 10.1 Hz), 5.32 (dd, 1H, CH═C*H*P, J = 17.6, 13.1 Hz), 3.90 (dd, 4H, CH_2P, J = 14.1, 3.3 Hz), 2.21 (s, 12H, CH_3), and 2.19 (s, 6H, CH_3) ppm. ^{31}P{^{1}H} NMR (161 MHz, DMSO-d_6) δ: 28.15 (s) and 25.13 (s) ppm. ^{13}C NMR (100 MHz, DMSO-d_6) δ: 197.13 (d, C═O, J = 4.1 Hz), 159.70 (d, HOCH═CH, J = 14.7 Hz), 141.26 (d, Ar-CP, J = 9.0 Hz), 140.95 (d, Ar-CP, J = 8.6 Hz), 134.41 (s, Ar-C), 133.39 (s, Ar-C), 132.65 (d, Ar-CH, J = 2.7 Hz), 132.28−130.76 (m, Ar-CH), 126.34 (d, Ar-CH, J = 12.2 Hz), 126.10 (d, Ar-CH, J = 12.0 Hz), 93.03 (d, CH═CHP, J = 116.02 Hz), 46.35 (d, CH_2P, J = 59.4 Hz), 21.05 (d, Ar-CH_3, J = 4.2 Hz), and 20.93 (d, Ar-CH_3, J = 4.5 Hz) ppm. ^{1}H NMR (400 MHz, CD_3OD) δ: 7.56−7.49 (m, 2H, Ar-H), 7.46−7.41 (m, 2H, Ar-H), 7.32−7.26 (m, 4H, Ar-H), 4.49 (dt, 1H, O-CH-O, J = 8.4, 5.2 Hz), 3.05−2.98 (m, 2H, P-CH_2-CH), and 2.33 (s, 6H, Ar-CH_3) ppm. ^{31}P{^{1}H} NMR (161 MHz, CD_3OD) δ: −21.04 (s) ppm. ^{13}C NMR (100 MHz, CD_3OD) δ: 142.52 (d, Ar-CP, J = 16.1 Hz), 135.58 (s, Ar-C), 132.63 (d, Ar-CH, J = 6.5 Hz), 132.19 (s, Ar-CH),131.03 (d, Ar-CH, J = 8.3 Hz), 126.56 (d, Ar-CH, J = 8.2 Hz), 101.00 (d, CHOO, J = 4.5 Hz), 26.99 (d, OOCHCH_2P, J = 25.8 Hz), and 19.58 (d, Ar-CH_3, J = 13.6 Hz) ppm. Anal. Calcd for $[C_{32}H_{36}O_2P_2][Br]_2 \cdot 0.25[H_2O]$: C, 56.24; H, 5.46, Found: C, 56.27; H, 5.35. MS (DART; m/z^+): 257.1 $[C_{32}H_{36}O_2P_2]^{2+}$. MS (ESI, methanol/water; m/z^+): 257.1 $[C_{16}H_{18}OP]^+$, 289.1 $[C_{19}H_{20}O_2P]^+$.

Synthesis of $[C_{36}H_{44}O_2P_2][Br]_2$ (2c). Similar to the synthesis of **2b**; see Supporting Information S2−S3.

Synthesis of $[C_{50}H_{52}N_4P_2Fe][B(C_6H_5)_4]_2$ (3a). A vial was charged with **2a** (0.235 g, 0.324 mmol) and CH_3CN (4 mL). A yellow solution of $[Fe(H_2O)_6][BF_4]_2$ (0.164 g, 0.485 mmol) in CH_3CN (2 mL) was added to the white slurry, followed by NaOMe (0.035 g, 0.647 mmol) in MeOH (1 mL). The color of the solution changed from yellow to colorless. After 20 min of stirring, (1*S*,2*S*)-(−)-1,2-diphenylethylenediamine (0.069 g, 0.323 mmol) in CH_3CN (0.5 mL) was added over 5 min, and the solution turned deep purple. After 48 h, the mixture was filtered to remove a white precipitate. The solvent was removed under reduced pressure to give a red-pink residue. The residue was dissolved in a minimum of MeOH (∼1 mL) and added to a solution of $NaBPh_4$ (0.250 g, 0.658 mmol) in MeOH (1 mL) to cause the precipitation of a pale pink solid. The product was filtered and washed with MeOH (2 × 5 mL) and dried under vacuum. Yield: 26.3% (0.120 g). Crystals suitable for X-ray diffraction studies were obtained by slow diffusion of Et_2O into CH_3CN/MeOH (1:5 by volume). ^{1}H NMR (400 MHz, CD_3CN) δ: 8.20−8.09 (m, 2H, HC═N), 7.75−6.80 (m, 66H, Ar-H), 5.42 (s, 2H, HC-N), 4.30−4.15 (m, 2H, HC-P), 4.03−3.90 (m, 2H, HC-P), 2.40 (s, 6H, Ar-CH_3), 2.35 (s, 6H, Ar-CH_3), and 1.53 (s, 6H, CH_3CN) ppm. ^{31}P{^{1}H} NMR (161 MHz; CD_3CN) δ: 72.42 (s) ppm. ^{13}C NMR (CD_3CN, 100 MHz) δ: 177.83 (C═NH), 164.08 (B-C), 143.05 (Ar-CP), 141.82 (Ar-CP), 136.01 (B−C-CH), 134.20 (Ar−CH), 134.11 (Ar-C), 131.74 (Ar-CH), 130.18 (Ar-CH), 129.90 (Ar-CH), 129.79 (Ar-C), 129.63 (Ar-CH), 125.87 (B-C-CH-CH), 122.04 (B-C-CH−CH-CH), 78.76 (CH-NH), 46.08 (CH_2-P), and 20.76 (Ar-CH_3) ppm. Anal. Calcd for $[C_{50}H_{52}N_4P_2Fe][B(C_6H_5)_4]_2$: C, 80.33; H, 6.33; N, 3.82. Found: C, 76.31; H, 6.71; N, 3.77. MS (ESI, methanol/water; m/z^+): 372.1 $[C_{50}H_{52}N_4P_2Fe]^{2+}$.

Synthesis of $[C_{50}H_{52}N_4P_2Fe][B(C_6H_5)_4]_2$ (3b). Similar to the synthesis of **3a**; see Supporting Information S3−S4.

Synthesis of $[C_{54}H_{60}N_4P_2Fe][B(C_6H_5)_4]_2$ (3c). Similar to the synthesis of **3a**; see Supporting Information S4−S5.

Synthesis of $[C_{20}H_{27}O_3P]$ (4a). A Schlenk flask was charged with KH (0.166 g, 4.13 mmol) and dry THF (8 mL). A solution of bis(*para*-tolyl)phosphine oxide (1.00 g, 4.13 mmol) in THF (8 mL) was added. Gas evolved, and the solution turned yellow. After 30 min of stirring, gas evolution ceased, and the solution was cooled to 0 °C. Bromoacetaldehyde diethyl acetal (0.725 g, 4.13 mmol) was added to the mixture over 5 min. The solution turned lighter yellow and cloudier. After 20 h, the solution was warmed to room temperature and ether (20 mL) was added. The solution was filtered, and the solvent was removed under reduced pressure to give a cloudy oil. The oil was dissolved in 3:1 hexanes/ether and cooled in a freezer (−40 °C) overnight. The solution was filtered, and the solvent removed under reduced pressure to give a clear, colorless oil. Yield: 54.6% (0.788 g). ^{1}H NMR (400 MHz, $CDCl_3$) δ: 7.66−7.59 (m, 4H, Ar−-H), 7.26−7.20 (m, 4H, Ar-H), 4.99 (q, 1H, O-CH-O, J = 5.5 Hz), 3.62−3.54 (m, 2H, O-CH_2), 3.45−3.37 (m, 2H, O-CH_2), 2.69 (dd, 2H, P-CH_2-CH, J = 11.4, 5.5 Hz), 2.38 (s, 6H, Ar-CH_3), and 0.99 (t, 6H, CH_2-CH_3, J = 7.0 Hz) ppm. ^{31}P{^{1}H} NMR ($CDCl_3$, 161 MHz) δ: 28.56 (s) ppm. ^{13}C NMR (100 MHz, $CDCl_3$) δ: 141.85 (d, Ar-CP, J = 2.9 Hz), 130.92 (s, Ar-CH), 130.83 (s, Ar-CH), 129.91 (s, Ar-C), 129.15 (s, Ar-CH), 129.03 (s, Ar-CH), 98.80 (s, CHOO), 62.44 (s, CH_2O), 36.16 (d, OOCHCH_2P, J = 71.3 Hz), 21.53 (d, Ar-CH_3, J = 1.3 Hz), and 14.94 (s, CH_3) ppm. Anal. Calcd for $[C_{20}H_{27}O_3P]$: C, 69.35; H, 7.86. Found: C, 69.08; H, 7.83. MS (DART, dichloromethane; m/z^+): 347.2 $[C_{20}H_{28}O_3P]^+$.

Synthesis of $[C_{20}H_{27}O_3P]$ (4b). Similar to the synthesis of **4a**; see Supporting Information S5−S6.

Synthesis of $[C_{22}H_{31}O_3P]$ (4c). Similar to the synthesis of **4a**; see Supporting Information S6.

Synthesis of $[C_{20}H_{27}O_2P]$ (5a). A Schlenk flask was charged with $LiAlH_4$ (0.204 g, 5.37 mmol) and dry ether (10 mL) and then cooled to 0 °C. A solution of **4a** (0.603 g, 1.74 mmol) in ether (5 mL) was added slowly. Gas evolved. After stirring for 45 min, the solution turned yellow and gas evolution ceased. The solution was stirred overnight and cooled to 0 °C, and degassed H_2O (0.20 mL) was added slowly. Gas evolved, and the solution turned clear with a gray precipitate. The solution was filtered, and the solvent was removed under reduced pressure, yielding a clear oil. Crude yield: 59.6% (0.343 g). Analytically pure samples were obtained from silica gel chromatography, eluting with 10:1 hexanes/ethyl acetate. ^{1}H NMR (300 MHz, CD_2Cl_2) δ: 7.33 (app t, 4H, Ar-H, J = 7.7 Hz), 7.15 (d, 4H, Ar-H, J = 7.7 Hz), 4.54 (q, 1H, O-CH-O, J = 5.9 Hz), 3.65−3.54 (m, 2H, O-CH_2), 3.50−3.38 (m, 2H, O-CH_2), 2.40 (d, 2H, P-CH_2-CH, J = 5.9 Hz), 2.34 (s, 6H, Ar-CH_3), and 1.12 (t, 6H, CH_3, J = 7.0 Hz) ppm. ^{31}P{^{1}H} NMR (161 MHz, CD_2Cl_2) δ: −24.40 (s) ppm. ^{13}C NMR (100 MHz, CD_2Cl_2) δ: 138.71 (s, Ar-C), 135.81 (d, Ar-CP, J = 12.1 Hz), 132.88 (d, Ar-CH, J = 19.7 Hz), 129.58 (d, Ar-CH, J = m 7.1 Hz), 101.44 (d, CHOO, J = 21.3 Hz), 61.40 (s, CH_2O), 34.18 (d, OOCHCH_2P, J = 14.1 Hz), 21.13 (s, Ar-CH_3), and 15.20 (s, CH_3) ppm. Anal. Calcd for $[C_{20}H_{27}O_2P]$: C, 72.70; H, 8.24. Found: C, 72.36; H, 8.23. MS (DART; m/z^+): 331.2 $[C_{20}H_{28}O_2P]^+$, 213.1$[C_{14}H_{14}P]^+$.

Synthesis of $[C_{20}H_{27}O_2P]$ (5b). Similar to the synthesis of **5a**; see Supporting Information S6−S7.

Synthesis of $[C_{22}H_{31}O_2P]$ (5c). Similar to the synthesis of **5a**; see Supporting Information S7.

Alternative Synthesis of $[C_{32}H_{36}O_2P_2][Br]_2$ (2a). A Schlenk flask was charged with **5a** (0.754 g, 2.28 mmol) and dry THF (5 mL). An excess of 48% HBr (0.60 mL, 7.20 mmol) was added. Over 5 min a white precipitate formed. The solution was stirred overnight and then cooled in a freezer (−40 °C) for 2 h. The white solid was filtered, washed with H_2O (10 mL) and ether (2 × 10 mL), and dried under high vacuum to yield a white powder. Yield: 86.7% (0.683 g). All spectroscopic data were identical to **2a**.

Synthesis of $[C_{32}H_{36}O_2P_2][BF_4]_2$ (6a). A Schlenk flask was charged with **5a** (0.823 g, 2.09 mmol) and dry THF (5 mL). An excess of 48% HBr (0.70 mL, 8.40 mmol) was added. Over 30 min a white precipitate formed. The solution was stirred overnight and then cooled in a freezer (−40 °C) for 5 h. The white solid was filtered, washed with H_2O (10 mL) and ether (2 × 10 mL), and dried under high vacuum to yield a white powder. Crystals suitable for X-ray diffraction studies were obtained from slow diffusion of ether into MeOH. Yield: 93.5% (0.804 g). All spectroscopic data were identical to **2a**. Anal. Calcd for $[C_{32}H_{36}O_2P_2][BF_4]_2 \cdot 1.5[H_2O]$: C, 53.74; H, 5.50. Found: C, 53.89; H, 5.17.

Alternative Synthesis of $[C_{32}H_{36}O_2P_2][Br]_2$ (2b). Similar to the alternative synthesis of **2a**; see Supporting Information S8.

Synthesis of $[C_{32}H_{36}O_2P_2][BF_4]_2$ (6b). Similar to the synthesis of **6a**; see Supporting Information S8.

Alternative Synthesis of $[C_{36}H_{44}O_2P_2][Br]_2$ (2c). Similar to the alternative synthesis of **2a**; see Supporting Information S8.

Synthesis of $[C_{36}H_{44}O_2P_2][BF_4]_2$ (6c). Similar to the synthesis of **6a**; see Supporting Information S8.

Alternative Synthesis of $[C_{50}H_{52}N_4P_2Fe][B(C_6H_5)_4]_2$ (3a). A vial was charged with **6a** (0.237 g, 0.324 mmol) and CH_3CN (4 mL). A yellow solution of $[Fe(H_2O)_6][BF_4]_2$ (0.109 g, 0.324 mmol) in CH_3CN (2 mL) was added to the white slurry, followed by NaOMe (0.035 g, 0.647 mmol) in CH_3CN (1 mL). The color of the solution changed from yellow to orange. After 20 min of stirring, (1*S*,2*S*)-(−)-1,2-diphenylethylenediamine (0.069 g, 0.323 mmol) in CH_3CN (0.5 mL) was added over 5 min, and the solution turned purple. After 48 h, the mixture was filtered to remove a white precipitate. The solvent was removed under reduced pressure to give an orange-red residue. The residue was dissolved in MeOH (∼2 mL) and added to a solution of $NaBPh_4$ (0.250 g, 0.658 mmol) in MeOH (1 mL) to cause precipitation of a pale pink solid. The product was filtered and washed with MeOH (2 × 5 mL) and dried under vacuum. Yield: 39.9% (0.182 g). All spectroscopic data were identical to **3a**.

Alternative Synthesis of $[C_{50}H_{52}N_4P_2Fe][B(C_6H_5)_4]_2$ (3b). Similar to the alternative synthesis of **3a**; see Supporting Information S8−S9.

Alternative Synthesis of $[C_{54}H_{60}N_4P_2Fe][B(C_6H_5)_4]_2$ (3c). Similar to the alternative synthesis of **3a**; see Supporting Information S9.

Synthesis of $[C_{20}H_{21}F_6O_2P]$ (5d). A Schlenk flask was charged with KH (0.079 g, 2.3 mmol) and dry THF (6 mL) and then cooled to −40 °C. Di(*para*-trifluoromethylphenyl)phosphine (0.473 g, 1.5 mmol) was added, and the mixture was stirred for 2 h, until the solution was dark red in color. Bromoacetaldehyde diethyl acetal (0.23 mL, 1.5 mmol) was added over 10 min. The solution was stirred for 30 min and then warmed to room temperature. The solution turned yellow-brown, and the solvent was removed under reduced pressure. The dark brown residue was dissolved in ether, filtered, and dried under high vacuum to yield a brownish-red oil. Yield: 72.0% (0.463 g). ^{1}H NMR (400 MHz, CD_2Cl_2) δ: 7.60−7.57 (m, 4H, Ar-H), 4.64 (t, 1H, O-CH-O, J= 5.5 Hz), 3.65−3.29 (m, 4H, O-CH_2), 2.95 (dd, 2H, P-CH_2-CH, J= 5.8, 0.75 Hz), and 1.10 (t, 3H, CH_3, J = 7.0 Hz) ppm. ^{31}P{^{1}H} NMR (161 MHz, CD_2Cl_2) δ: −22.03 (s) ppm. ^{19}F NMR (376 MHz, CD_2Cl_2) δ: −63.20 (s) ppm. ^{13}C NMR (100 MHz, CD_2Cl_2) δ: 143.6 (app d, Ar-C), 133.12 (d Ar-CH, J = 19.5 Hz,), 130.43 (d, Ar-CP, J = 32.4 Hz), 124.99 (app sept, Ar-CH), 100.37 (d, CHOO, J = 21.1 Hz), 61.70 (s, CH_2O), 33.75 (d, OOCHCH_2P, J = 14.9 Hz), and 14.87 (s, CH_3) ppm. Anal. Calcd for $[C_{20}H_{21}F_6O_2P]$: C, 54.80; H, 4.83. Found: C, 54.69; H, 4.76. MS (EI, dichloromethane; m/z^+): 438.1 $[C_{20}H_{21}F_6O_2P]^+$, 392.1 $[C_{18}H_{15}F_6OP]^+$, 322.0 $[C_{14}H_9F_6P]^+$.

Synthesis of $[C_{22}H_{19}F_{12}O_2P]$ (5e). Similar to the synthesis of **5d**; see Supporting Information S9−S10.

Synthesis of $[C_{50}H_{40}F_{16}FeN_4P_2][BF_4]_2$ (3d). A Schlenk flask was charged with **5d** (0.284 g, 0.646 mmol), $[Fe(H_2O)_6][BF_4]_2$ (0.109 g, 0.324 mmol), and CH_3CN (4 mL). The yellow solution was left for 1 h, and it turned darker in color. (1*S*,2*S*)-(−)-1,2-Diphenylethylenediamine (0.069 mg, 0.323 mmol) in CH_3CN (2 mL) was added, and the solution was left for 6 h. The solution slowly turned pink. A small amount of 48% HBF_4 (0.1 mL, 1.2 mmol) was added, and the solution was stirred for 6 h. The solution turned cloudy and colorless. The solvent was removed under reduced pressure to give a pale yellow residue. The residue was dissolved in CH_3CN (4 mL), and a slurry of NaOMe (0.065 g, 1.2 mmol) in CH_3CN (2 mL) was added, along with 4 drops of MeOH. The solution turned dark red over 20 min. The solution was stirred overnight and then filtered. The solvent was removed under reduced pressure, and the red residue was dissolved in a minimum of CH_2Cl_2 (∼5 mL) and then filtered. The solvent was removed under reduced pressure, and the red solid was washed with 5:1 ether/THF (2 × 5 mL). Yield: 44.2% (0.174 g). ^{1}H NMR (400 MHz, CD_3CN) δ: 8.30−8.15 (m, 2H, HC═N), 7.85 (app d, 4H, Ar-H), 7.67 (app d, 4H, Ar-H), 7.51 (app q, 8H, Ar-H), 7.43 (s, 10H, dpen Ar-H), 5.48 (s, 2H, HC-N), 4.54−4.40 (m, 2H, HC-P), 4.34−4.20 (m, 2H, HC-P), and 1.71 (s, 6H, CH_3CN) ppm. ^{31}P{^{1}H} NMR (161 MHz, CD_3CN) δ: 69.01 (s) ppm. ^{19}F NMR (376 MHz, CD_3CN) δ: −63.74 (s) and −63.87 (s) ppm. ^{13}C NMR (100 MHz, CD_3CN) δ: 178.53 (C═NH), 137.92 (CH_3CN), 137.3 (CF_3), 134.78 (Ar-CH), 133.88 (Ar-C), 132.72 (Ar-CH), 130.27 (Ar-C), 132.24 (CF_3), 129.96 (Ar-C), 129.61 (Ar-CH), 126.31 (Ar-CH), 126.05 (Ar-CH), 125.32 (Ar-CP), 78.72 (CH-NH), 45.31 (CH_2P), and 4.53 (CH_3CN) ppm. Anal. Calcd for $[C_{50}H_{40}F_{16}FeN_4P_2][BF_4]_2$: C, 49.38; H, 3.31; N, 4.61. Found: C, 44.70; H, 3.53; N, 4.06. MS (ESI, dichloromethane; m/z^+): 480.2 $[C_{46}H_{34}F_{12}FeN_2P_2]^{2+}$.

Synthesis of $[C_{54}H_{36}F_{24}FeN_4P_2][BF_4]_2$ (3e). Similar to the synthesis of **3d**; see Supporting Information S10−S11.

Synthesis of $[C_{53}H_{26}BrFeN_2OP_2][B(C_6H_5)_4]$ (1a). The crude reaction mixture of **2a** (either starting with the bromide or tetrafluoroborate phosphonium dimer) was filtered. The solvent was removed under reduced pressure, and acetone (9 mL) was added, along with an excess of KBr. The solution was stirred under a CO headspace for 3 days. The resulting yellow-brown solution was evaporated to dryness, dissolved in a minimum of MeOH (∼2 mL), filtered, and added to a solution of $NaBPh_4$ (0.125 g, 0.329 mmol) in MeOH (1 mL) to cause the formation of a yellow precipitate. The precipitate was washed with ether (2 × 5 mL) and MeOH (5 mL) and dried under high vacuum. Yield: 28.5% (0.108 g). ^{1}H NMR (400 MHz, $(CD_3)_2CO$) δ: 7.81−7.72 (m, 1H, HC═N), 7.67−7.58 (m, 1H, HC═N), 7.32−6.71 (m, 46H, Ar-H), 5.68−5.61 (m, 1H, HC-N), 5.18−5.11 (m, 1H, HC-N), 4.09−3.99 (m, 1H, HC-P), 3.82−3.70 (m, 2H, HC-P), 3.62−3.52 (m, 1H, HC-P), 2.34 (s, 3H, Ar-CH_3), 2.33 (s, 3H, Ar-CH_3), 2.30 (s, 3H, Ar-CH_3), and 2.26 (s, 3H, Ar-CH_3) ppm. ^{31}P{^{1}H} NMR (161 MHz, $(CD_3)_2CO$) δ: 65.96 (d, J = 39.5 Hz) and 67.93 (d, J = 39.5 Hz) ppm. ^{13}C NMR (100 MHz, $(CD_3)_2CO$) δ: 175.00 (C═NH), 174.74 (C═NH), 164.04 (B-C), 142.39 (Ar-CP), 141.95 (Ar-CP), 141.25 (Ar-CP), 140.94 (Ar-CP), 136.12 (B-C-CH), 134.96 (Ar-C), 134.86 (Ar-C), 134.27 (Ar-C), 134.10 (Ar-C), 133.73 (Ar-CH), 133.62 (Ar-CH), 133.57 (Ar-CH), 133.48 (Ar-CH), 131.34 (Ar-C), 131.25 (Ar-C), 129.82 (Ar-CH),129.75 (Ar-CH), 129.48 (Ar-CH), 129.43 (Ar-CH), 129.40 (Ar-CH), 129.38 (Ar-CH), 129.33 (Ar-CH), 129.31 (Ar-CH), 129.29 (Ar-CH), 128.99 (Ar-CH), 128.89 (Ar-CH), 128.32 (Ar-CH), 128.21(Ar-CH), 125.06 (B-C-CH-CH), 121.30 (B-C-CH-CH-CH), 80.24 (CH-NH), 77.60 (CH-NH), 47.56 (CH_2-P), 47.27 (CH_2-P),

dx.doi.org/10.1021/om2005172 |*Organometallics* 2011, 30, 4418–4431

and 20.50 (Ar-CH_3) ppm. IR (KBr): 1972 cm^{-1} ($\nu_{C\equiv O}$). Anal. Calcd for $[C_{53}H_{26}BrFeN_2OP_2][B(C_6H_5)_4]$: C, 72.71; H, 5.68; N, 2.39. Found: C, 70.72; H, 5.99; N, 2.11. MS (ESI, dichloromethane; m/z^+): 851.2 $[C_{47}H_{46}BrFeN_2OP_2]^+$.

Synthesis of $[C_{53}H_{26}BrFeN_2OP_2][B(C_6H_5)_4]$ (1b). Similar to the synthesis of **1a**; see Supporting Information S11−S12.

Synthesis of $[C_{51}H_{54}BrFeN_2OP_2][B(C_6H_5)_4]$ (1c). Similar to the synthesis of **1a**; see Supporting Information S12.

Synthesis of $[C_{47}H_{34}BrF_{12}FeN_2OP_2][BF_4]$ (1d). Similar to the synthesis of **1a**; see Supporting Information S13.

Synthesis of $[C_{51}H_{30}F_{24}BrFeN_2OP_2][BF_4]$ (1e). Similar to the synthesis of **1a**; see Supporting Information S13−S14.

■ ASSOCIATED CONTENT

Supporting Information. Extended experimental section. Crystal structures and crystallographic data for **3b**, **4b**, **6a**, **6c**, and **7** (including CIF files). Sample calculations for Tolman cone angles. Catalytic and GC conditions for ATH of acetophenone and TH of benzophenone. Catalytic profiles for TH of benzophenone for **1a** and **1c**. Comparison of the linear portions of the catalytic profiles for **1a** and **1c**. This material is available free of charge via the Internet at http://pubs.acs.org.

■ AUTHOR INFORMATION

Corresponding Author

*E-mail: rmorris@chem.utoronto.ca.

■ ACKNOWLEDGMENT

We thank NSERC Canada for a Discovery grant to R.H.M

■ REFERENCES

(1) Gaillard, S.; Renaud, J.-L. *ChemSusChem* **2008**, *1*, 505–509.
(2) Oldenburg, P. D.; Que, J. L. *Catal. Today* **2006**, *117*, 15–21.
(3) Yeung, H.-L.; Sham, K.-C.; Tsang, C.-S.; Lau, T.-C.; Kwong, H.-L. *Chem. Commun.* **2008**, 3801–3803.
(4) Bruijnincx, P. C. A.; Buurmans, I. L. C.; Gosiewska, S.; Moelands, M. A. H.; Lutz, M.; Spek, A. L.; van Koten, G.; Klein Gebbink, R. J. M. *Chem.—Eur. J.* **2008**, *14*, 1228–1237.
(5) Suzuki, K.; Oldenburg, P. D.; Que, L. *Angew. Chem., Int. Ed.* **2008**, *47*, 1887–1889.
(6) Gómez, L.; Garcia-Bosch, I.; Company, A.; Benet-Buchholz, J.; Polo, A.; Sala, X.; Ribas, X.; Costas, M. *Angew. Chem., Int. Ed.* **2009**, *48*, 5720–5723.
(7) Muthupandi, P.; Alamsetti, S. K.; Sekar, G. *Chem. Commun.* **2009**, 3288–3290.
(8) Rose, E.; Ren, Q.-Z.; Andrioletti, B. *Chem.—Eur. J.* **2004**, *10*, 224–230.
(9) Ellis, W. C.; Tran, C. T.; Denardo, M. A.; Fischer, A.; Ryabov, A. D.; Collins, T. J. *J. Am. Chem. Soc.* **2009**, *131*, 18052–18053.
(10) Ellis, W. C.; Tran, C. T.; Roy, R.; Rusten, M.; Fischer, A.; Ryabov, A. D.; Blumberg, B.; Collins, T. J. *J. Am. Chem. Soc.* **2010**, *132*, 9774–9781.
(11) Popescu, D.-L.; Chanda, A.; Stadler, M. J.; Mondal, S.; Tehranchi, J.; Ryabov, A. D.; Collins, T. J. *J. Am. Chem. Soc.* **2008**, *130*, 12260–12261.
(12) Morris, R. H. *Chem. Soc. Rev.* **2009**, *38*, 2282–2291.
(13) Junge, K.; Schroder, K.; Beller, M. *Chem. Commun.* **2011**, *47*, 4849–4859.
(14) Tondreau, A. M.; Lobkovsky, E.; Chirik, P. J. *Org. Lett.* **2008**, *10*, 2789–2792.
(15) Tondreau, A. M.; Darmon, J. M.; Wile, B. M.; Floyd, S. K.; Lobkovsky, E.; Chirik, P. J. *Organometallics* **2009**, *28*, 3928–3940.
(16) Casey, C. P.; Guan, H. *J. Am. Chem. Soc.* **2007**, *129*, 5816–5817.
(17) Langer, R.; Leitus, G.; Ben-David, Y.; Milstein, D. *Angew. Chem., Int. Ed.* **2011**, *50*, 2120–2124.
(18) Kandepi, V. V. K. M.; Cardoso, J. M. S.; Peris, E.; Royo, B. *Organometallics* **2010**, *29*, 2777–2782.
(19) Naik, A.; Maji, T.; Reiser, O. *Chem. Commun.* **2010**, *46*, 4475–4477.
(20) Enthaler, S.; Erre, G.; Tse, M. K.; Junge, K.; Beller, M. *Tetrahedron Lett.* **2006**, *47*, 8095–8099.
(21) Buchard, A.; Heuclin, H.; Auffrant, A.; Le Goff, X. F.; Le Floch, P. *Dalton Trans.* **2009**, 1659–1667.
(22) Enthaler, S.; Hagemann, B.; Erre, G.; Junge, K.; Beller, M. *Chem. Asian J.* **2006**, *1*, 598–604.
(23) Mashima, K.; Abe, T.; Tani, K. *Chem. Lett.* **1998**, *27*, 1199–1200.
(24) Sui-Seng, C.; Freutel, F.; Lough, A. J.; Morris, R. H. *Angew. Chem., Int. Ed.* **2008**, *47*, 940–943.
(25) Zhou, S.; Fleischer, S.; Junge, K.; Das, S.; Addis, D.; Beller, M. *Angew. Chem., Int. Ed.* **2010**, *49*, 8121–8125.
(26) Blaser, H.-U.; Studer, M. *Acc. Chem. Res.* **2007**, *40*, 1348–1356.
(27) Klingler, F. D. *Acc. Chem. Res.* **2007**, *40*, 1367–1376.
(28) Ikariya, T.; Blacker, A. J. *Acc. Chem. Res.* **2007**, *40*, 1300–1308.
(29) Noyori, R.; Ohkuma, T. *Angew. Chem., Int. Ed.* **2001**, *40*, 40–73.
(30) Dong, Z.-R.; Li, Y.-Y.; Chen, J.-S.; Li, B.-Z.; Xing, Y.; Gao, J.-X. *Org. Lett.* **2005**, *7*, 1043–1045.
(31) Li, Y.-Y.; Zhang, X.-Q.; Dong, Z.-R.; Shen, W.-Y.; Chen, G.; Gao, J.-X. *Org. Lett.* **2006**, *8*, 5565–5567.
(32) Gao, J.-X.; Ikariya, T.; Noyori, R. *Organometallics* **1996**, *15*, 1087–1089.
(33) Mikhailine, A.; Lough, A. J.; Morris, R. H. *J. Am. Chem. Soc.* **2009**, *131*, 1394–1395.
(34) Mikhailine, A. A.; Morris, R. H. *Inorg. Chem.* **2010**, *49*, 11039–11044.
(35) Lagaditis, P. O.; Lough, A. J.; Morris, R. H. *Inorg. Chem.* **2010**, *49*, 10057–10066.
(36) Guo, R.; Chen, X.; Elpelt, C.; Song, D.; Morris, R. H. *Org. Lett.* **2005**, *7*, 1757–1759.
(37) Moser, W. R.; Papile, C. J.; Brannon, D. A.; Duwell, R. A.; Weininger, S. J. *J. Mol. Catal.* **1987**, *41*, 271–292.
(38) Palo, D. R.; Erkey, C. *Organometallics* **1999**, *19*, 81–86.
(39) Wang, X.; Lane, B. S.; Sames, D. *J. Am. Chem. Soc.* **2005**, *127*, 4996–4997.
(40) Muller, J. G.; Acquaye, J. H.; Takeuchi, K. J. *Inorg. Chem.* **1992**, *31*, 4552–4557.
(41) Casalnuovo, A. L.; RajanBabu, T. V.; Ayers, T. A.; Warren, T. H. *J. Am. Chem. Soc.* **1994**, *116*, 9869–9882.
(42) Mikhailine, A. A.; Lagaditis, P. O.; Sues, P. E.; Lough, A. J.; Morris, R. H. *J. Organomet. Chem.* **2010**, *695*, 1824–1830.
(43) Lagaditis, P. O.; Mikhailine, A. A.; Lough, A. J.; Morris, R. H. *Inorg. Chem.* **2009**, *49*, 1094–1102.
(44) Busacca, C. A.; Lorenz, J. C.; Grinberg, N.; Haddad, N.; Hrapchak, M.; Latli, B.; Lee, H.; Sabila, P.; Saha, A.; Sarvestani, M.; Shen, S.; Varsolona, R.; Wei, X.; Senanayake, C. H. *Org. Lett.* **2005**, *7*, 4277–4280.
(45) Matt, D.; Ziessel, R.; De Cian, A.; Fischer, J. *New J. Chem.* **1996**, *20*, 1257–1263.
(46) Mikhailine, A. A.; Kim, E.; Dingels, C.; Lough, A. J.; Morris, R. H. *Inorg. Chem.* **2008**, *47*, 6587–6589.
(47) Mizoshita, N.; Tani, T.; Inagaki, S. *Chem. Soc. Rev.* **2011**, *40*, 789–800.
(48) Busch, D. H.; Stephenson, N. A. *Coord. Chem. Rev.* **1990**, *100*, 119–154.
(49) Battle, A. R.; Edwards, P. G.; Haigh, R.; Hibbs, D. E.; Li, D.; Liddiard, S. M.; Newman, P. D. *Organometallics* **2006**, *26*, 377–386.
(50) Albers, T.; Edwards, P. G. *Chem. Commun.* **2007**, 858–860.
(51) Doering, W. V. E.; Young, R. W. *J. Am. Chem. Soc.* **1950**, *72*, 631–631.
(52) Tolman, C. A. *Chem. Rev.* **1977**, *77*, 313–348.

(53) Fernandez, A. L.; Reyes, C.; Prock, A.; Giering, W. P. *J. Chem. Soc., Perkin Trans. 2* **2000**, 1033–1041.
(54) Bunten, K. A.; Moreno, C.; Poe, A. J. *Dalton Trans.* **2005**, 1416–1421.
(55) Lagaditis, P. O.; Lough, A. J.; Morris, R. H. *J. Am. Chem. Soc.* **2011**, *133*, 9662–9665.
(56) Hashiguchi, S.; Fujii, A.; Takehara, J.; Ikariya, T.; Noyori, R. *J. Am. Chem. Soc.* **1995**, *117*, 7562–7563.
(57) Takehara, J.; Hashiguchi, S.; Fujii, A.; Inoue, S.-I.; Ikariya, T.; Noyori, R. *Chem. Commun.* **1996**, 233–234.
(58) Alonso, D. A.; Nordin, S. J. M.; Roth, P.; Tarnai, T.; Andersson, P. G.; Thommen, M.; Pittelkow, U. *J. Org. Chem.* **2000**, *65*, 3116–3122.
(59) Palmer, M. J.; Kenny, J. A.; Walsgrove, T.; Kawamoto, A. M.; Wills, M. *J. Chem. Soc. Perkin Trans. 1* **2002**, 416–427.
(60) Hannedouche, J.; Clarkson, G. J.; Wills, M. *J. Am. Chem. Soc.* **2004**, *126*, 986–987.
(61) Murata, K.; Ikariya, T.; Noyori, R. *J. Org. Chem.* **1999**, *64*, 2186–2187.
(62) Bubert, C.; Blacker, J.; Brown, S. M.; Crosby, J.; Fitzjohn, S.; Muxworthy, J. P.; Thorpe, T.; Williams, J. M. J. *Tetrahedron Lett.* **2001**, *42*, 4037–4039.
(63) Guo, R.; Elpelt, C.; Chen, X.; Song, D.; Morris, R. H. *Chem. Commun.* **2005**, 3050–3052.
(64) Bligaard, T.; Nørskov, J. K.; Dahl, S.; Matthiesen, J.; Christensen, C. H.; Sehested, J. *J. Catal.* **2004**, *224*, 206–217.
(65) Cheng, J.; Hu, P. *J. Am. Chem. Soc.* **2008**, *130*, 10868–10869.
(66) Jacobsen, C. J. H.; Dahl, S.; Clausen, B. S.; Bahn, S.; Logadottir, A.; Nørskov, J. K. *J. Am. Chem. Soc.* **2001**, *123*, 8404–8405.
(67) RajanBabu, T. V.; Ayers, T. A.; Halliday, G. A.; You, K. K.; Calabrese, J. C. *J. Org. Chem.* **1997**, *62*, 6012–6028.
(68) RajanBabu, T. V.; Radetich, B.; You, K. K.; Ayers, T. A.; Casalnuovo, A. L.; Calabrese, J. C. *J. Org. Chem.* **1999**, *64*, 3429–3447.
(69) Yan, Y.-Y.; RajanBabu, T. V. *J. Org. Chem.* **2001**, *66*, 3277–3283.
(70) Snelders, D. J. M.; van Koten, G.; Klein Gebbink, R. J. M. *Chem.—Eur. J.* **2011**, *17*, 42–57.
(71) Mikhailine, A. A.; Lagaditis, P. O.; Sues, P. E.; Lough, A. J.; Morris, R. H. *J. Organomet. Chem.* **2010**, *695*, 1824—1830.
(72) Marcó, A.; Compañó, R.; Rubio, R.; Casals, I. *Microchim. Acta* **2003**, *142*, 13–19.